

Towards a detection of reactor $\bar{\nu}_e \rightarrow \bar{\nu}_\mu$ and $\bar{\nu}_e \rightarrow \bar{\nu}_\tau$ oscillations with possible CP violation*

Yifang Wang (王贻芳)^{1,2†} Zhi-zhong Xing (邢志忠)^{1,2‡} Shun Zhou (周顺)^{1,2§}

¹Institute of High Energy Physics, Chinese Academy of Sciences, Beijing 100049, China

²University of Chinese Academy of Sciences, Beijing 100049, China

Abstract: We propose a novel method to detect reactor $\bar{\nu}_e \rightarrow \bar{\nu}_\mu$ and $\bar{\nu}_e \rightarrow \bar{\nu}_\tau$ oscillations by using elastic antineutrino-electron scattering processes $\bar{\nu}_\alpha + e^- \rightarrow \bar{\nu}_\alpha + e^-$ (for $\alpha = e, \mu, \tau$), among which the $\bar{\nu}_e$ events can be singled out by accurately measuring the $\bar{\nu}_e$ flux via the inverse beta decay $\bar{\nu}_e + p \rightarrow e^+ + n$. A proof-of-concept study shows that such measurements will not only be able to test the conservation of probability for reactor antineutrino oscillations, but also offer a new possibility to probe leptonic CP violation at the one-loop level.

Keywords: Neutrino Oscillations, Reactor Antineutrinos, CP Violation

DOI: CSTR:

I. INTRODUCTION

The reactor-based neutrino experiments have played a crucial role in the developments of nuclear and particle physics [1, 2], such as the discovery of the electron antineutrino $\bar{\nu}_e$ [3], the discoveries of long- and short-baseline $\bar{\nu}_e \rightarrow \bar{\nu}_e$ oscillations [4, 5], and the first measurement of the smallest lepton flavor mixing angles θ_{13} [5, 6]. The new flagship reactor neutrino oscillation experiment JUNO [7, 8], a medium-baseline facility which has just started data taking, aims to resolve another fundamental issue in particle physics and cosmology — the mass ordering of three active neutrinos.

It is well known that the flavor oscillations of reactor antineutrinos belong to the *disappearance* category, in the sense that the $\bar{\nu}_e$ events observed at the far detector are somewhat fewer than those recorded at the near detector. Although $\bar{\nu}_e \rightarrow \bar{\nu}_\mu$ and $\bar{\nu}_e \rightarrow \bar{\nu}_\tau$ oscillations *do* take place in a reactor experiment, they cannot be directly detected via the corresponding weak *charged-current* interactions associated with $\bar{\nu}_\mu$ and $\bar{\nu}_\tau$ [9]. The reason is simply that the reactor antineutrino beam energy is too low to produce the μ^+ or τ^+ events via the $\bar{\nu}_\mu + p \rightarrow \mu^+ + n$ or $\bar{\nu}_\tau + p \rightarrow \tau^+ + n$ processes in the detector. A burning question is therefore whether there exists a way out of this impasse in the coming precision measurement era.

The answer to this important question will be affirmative, if a dedicated measurement of the appearance of $\bar{\nu}_\mu$ and $\bar{\nu}_\tau$ events can be done by means of their weak *neutral-current* interactions with the target material. In this note we are going to propose a novel method to detect the reactor $\bar{\nu}_e \rightarrow \bar{\nu}_\mu$ and $\bar{\nu}_e \rightarrow \bar{\nu}_\tau$ oscillations with the help of elastic antineutrino-electron scattering processes $\bar{\nu}_\alpha + e^- \rightarrow \bar{\nu}_\alpha + e^-$ (for $\alpha = e, \mu, \tau$), among which the $\bar{\nu}_e$ events can be singled out by detecting the $\bar{\nu}_e$ flux via the inverse beta decay $\bar{\nu}_e + p \rightarrow e^+ + n$ to a sufficiently high degree of accuracy. We find that such precision measurements will help open a new window for experimental neutrino physics at least in the following three aspects:

1. to directly confirm the appearance of $\bar{\nu}_\mu$ and $\bar{\nu}_\tau$ events originating from the initial $\bar{\nu}_e$ events of a nuclear reactor via flavor oscillations, and thus to test the conservation of probability for reactor antineutrino oscillations by combining it with the $\bar{\nu}_e \rightarrow \bar{\nu}_e$ disappearance.

2. to probe a fine difference between $\bar{\nu}_e \rightarrow \bar{\nu}_\mu$ and $\bar{\nu}_e \rightarrow \bar{\nu}_\tau$ oscillations, which is sensitive to both the μ - τ interchange symmetry and the leptonic CP violation, by precisely measuring the cross sections of elastic $\bar{\nu}_\mu$ - e^- and $\bar{\nu}_\tau$ - e^- scattering reactions at the *one-loop* level.

Received 4 September 2025; Accepted 19 September 2025

* This work was supported in part by the National Natural Science Foundation of China under grant No. 12475113, the CAS Project for Young Scientists in Basic Research (YSBR-099), and the Scientific and Technological Innovation Program of IHEP under grant No. E55457U2

† E-mail: yfwang@ihep.ac.cn

‡ E-mail: xingzz@ihep.ac.cn

§ E-mail: zhoush@ihep.ac.cn



Content from this work may be used under the terms of the Creative Commons Attribution 3.0 licence. Any further distribution of this work must maintain attribution to the author(s) and the title of the work, journal citation and DOI. Article funded by SCOAP³ and published under licence by Chinese Physical Society and the Institute of High Energy Physics of the Chinese Academy of Sciences and the Institute of Modern Physics of the Chinese Academy of Sciences and IOP Publishing Ltd

3. to search for possible new physics either beyond the standard weak interactions or beyond the standard three-flavor oscillation scheme, or both of them.

We expect that the experimental and theoretical studies of this kind will find more applications at the low-energy luminosity or intensity frontiers of particle physics.

The present work is intended to provide a *proof-of-concept* investigation of points 1 and 2 listed above, with a very preliminary numerical illustration by taking the

JUNO experiment for example. In particular, we highlight the novel possibility of probing or constraining the leptonic CP-violating phase from a precision measurement of the reactor $\bar{\nu}_e \rightarrow \bar{\nu}_\mu$ and $\bar{\nu}_e \rightarrow \bar{\nu}_\tau$ oscillations.

II. FLAVOR OSCILLATIONS

Let us focus on the standard three-flavor oscillation scheme, in which the 3×3 unitary Pontecorvo-Maki-Nakagawa-Sakata (PMNS) neutrino mixing matrix U [10, 11] can be parameterized as¹⁾

$$U = \begin{pmatrix} U_{e1} & U_{e2} & U_{e3} \\ U_{\mu 1} & U_{\mu 2} & U_{\mu 3} \\ U_{\tau 1} & U_{\tau 2} & U_{\tau 3} \end{pmatrix} = \begin{pmatrix} c_{12}c_{13} & s_{12}c_{13} & \hat{s}_{13}^* \\ -s_{12}c_{23} - c_{12}\hat{s}_{13}s_{23} & c_{12}c_{23} - s_{12}\hat{s}_{13}s_{23} & c_{13}s_{23} \\ s_{12}s_{23} - c_{12}\hat{s}_{13}c_{23} & -c_{12}s_{23} - s_{12}\hat{s}_{13}c_{23} & c_{13}c_{23} \end{pmatrix}, \quad (1)$$

where $c_{ij} \equiv \cos \theta_{ij}$, $s_{ij} \equiv \sin \theta_{ij}$ and $\hat{s}_{13} \equiv s_{13}e^{i\delta}$ with θ_{ij} (for $ij = 12, 13, 23$) being the flavor mixing angles and δ being the nontrivial phase responsible for leptonic CP violation in neutrino oscillations. The probabilities of reactor $\bar{\nu}_e \rightarrow \bar{\nu}_\alpha$ oscillations in vacuum are given by

$$P(\bar{\nu}_e \rightarrow \bar{\nu}_\alpha) = \delta_{e\alpha} - 4 \sum_{i < j} \text{Re}(U_{ei}U_{ej}^*U_{\alpha i}^*U_{\alpha j}) \sin^2 F_{ji} - 8\mathcal{J} \sum_{\beta} \epsilon_{e\alpha\beta} \prod_{i < j} \sin F_{ji}, \quad (2)$$

where $F_{ji} \equiv (m_j^2 - m_i^2)L/(4E)$ with $m_{i,j}$ being the neutrino masses are defined (for $i, j = 1, 2, 3$), E represents the av-

erage antineutrino beam energy, L denotes the baseline length, $\epsilon_{e\alpha\beta}$ stands for the three-dimensional Levi-Civita symbol (for $\alpha, \beta = e, \mu, \tau$), and

$$\mathcal{J} = \frac{1}{8} \sin 2\theta_{12} \sin 2\theta_{13} \cos \theta_{13} \sin 2\theta_{23} \sin \delta \quad (3)$$

is the unique Jarlskog invariant of CP violation for the PMNS lepton flavor mixing matrix [13, 14].

It is obvious that the *disappearance* oscillation channel $\bar{\nu}_e \rightarrow \bar{\nu}_e$ is CP-conserving, while the *appearance* oscillation channels $\bar{\nu}_e \rightarrow \bar{\nu}_\mu$ and $\bar{\nu}_e \rightarrow \bar{\nu}_\tau$ contain the CP-violating terms of the same magnitude but the opposite signs. That is why we find it useful to redefine

$$P_+ \equiv P(\bar{\nu}_e \rightarrow \bar{\nu}_\mu) + P(\bar{\nu}_e \rightarrow \bar{\nu}_\tau) = 1 - P(\bar{\nu}_e \rightarrow \bar{\nu}_e) = 4 \sum_{i < j} |U_{ei}|^2 |U_{ej}|^2 \sin^2 F_{ji},$$

$$P_- \equiv P(\bar{\nu}_e \rightarrow \bar{\nu}_\mu) - P(\bar{\nu}_e \rightarrow \bar{\nu}_\tau) = \sum_{i < j} D_{ij} \sin^2 F_{ji} - 16\mathcal{J} \prod_{i < j} \sin F_{ji}, \quad (4)$$

where $D_{ij} \equiv 4\text{Re}[U_{ei}U_{ej}^*(U_{\tau i}^*U_{\tau j} - U_{\mu i}^*U_{\mu j})]$ characterize the effects of μ - τ interchange symmetry breaking for the PMNS matrix U . To be explicit, we obtain

$$D_{12} = +\sin^2 2\theta_{12} \cos^2 \theta_{13} \cos 2\theta_{23} (1 + \sin^2 \theta_{13} + 2 \cot 2\theta_{12} \sin \theta_{13} \tan 2\theta_{23} \cos \delta),$$

$$D_{13} = -2 \cos^2 \theta_{12} \sin 2\theta_{13} \cos \theta_{13} \cos 2\theta_{23} (\sin \theta_{13} - \tan \theta_{12} \tan 2\theta_{23} \cos \delta),$$

$$D_{23} = -2 \sin^2 \theta_{12} \sin 2\theta_{13} \cos \theta_{13} \cos 2\theta_{23} (\sin \theta_{13} + \cot \theta_{12} \tan 2\theta_{23} \cos \delta), \quad (5)$$

1) Possible non-unitarity of U has been constrained to be below $O(10^{-3})$ in the canonical seesaw mechanism [12], and thus can be neglected in this work. Here the Majorana phases of U are not taken into account either, as they are insensitive to the reactor antineutrino oscillations under discussion.

which will vanish in the limit of the μ - τ permutation symmetry (i.e., $\theta_{23} = \pi/4$ and $\theta_{13} = 0$) or the μ - τ reflection symmetry (i.e., $\theta_{23} = \pi/4$ and $\delta = \pm\pi/2$) [15]. Given the facts that the best-fit value of θ_{23} is really not far away from $\pi/4$ and the maximum value of $|\mathcal{J}|$ is about 3% in a global analysis of current neutrino oscillation data [16, 17], we conclude that the magnitudes of D_{ij} and \mathcal{J} are both suppressed, leading to an unfortunate suppression of P_- as compared with P_+ .

Note that the reactor $\bar{\nu}_e \rightarrow \bar{\nu}_e$ oscillations have been firmly established by measuring the survival $\bar{\nu}_e$ events at the far detector with the help of the weak charged-current $\bar{\nu}_e + p \rightarrow e^+ + n$ reactions. The first purpose of this work is to propose a careful precision measurement of P_+ by use of elastic $\bar{\nu}_\alpha + e^- \rightarrow \bar{\nu}_\alpha + e^-$ scattering (for $\alpha = \mu, \tau$) via the weak neutral-current interactions in a reactor-based experiment like the JUNO, such that one may effectively test the consistency of the standard three-flavor neutrino oscillation framework by examining the conservation of probability associated with these pure quantum processes [i.e., $P_+ + P(\bar{\nu}_e \rightarrow \bar{\nu}_e) = 1$ should hold].

For the sake of illustration, we show the probabilities P_+ and $P(\bar{\nu}_e \rightarrow \bar{\nu}_e)$ changing with the reactor antineutrino beam energy E in the left panel of Fig. 1, where $L = 53$ km has been taken as a typical baseline length. In addition, the best-fit values of the oscillation parameters $\sin^2 \theta_{12} = 0.308$, $\sin^2 \theta_{13} = 0.02215$, $\sin^2 \theta_{23} = 0.470$ and $\delta = 1.17\pi$, together with $m_2^2 - m_1^2 = 7.49 \times 10^{-5} \text{ eV}^2$ and $m_3^2 - m_1^2 = 2.513 \times 10^{-3} \text{ eV}^2$ (normal mass ordering) are taken from Ref. [16], where a perfect agreement with the results from an independent global-fit analysis of neutrino oscillation data in Ref. [17] can be found. From Fig. 1, it is clear that a significant fraction of the $\bar{\nu}_e$ events oscillate into the $\bar{\nu}_\mu$ and $\bar{\nu}_\tau$ events, especially in the energy range $E \in [2, 6] \text{ MeV}$. One may therefore expect that the antineutrinos of all three flavors are detectable in a liquid-scintillator detector.

In comparison, it is certainly more ambitious and thus more challenging to detect P_- by means of the same techniques, so as to probe or constrain the highly nontrivial effects of leptonic CP violation and μ - τ interchange symmetry breaking. The right panel of Fig. 1 illustrates how small P_- is expected to be with respect to P_+ . A delicate measurement of the cross sections of elastic $\bar{\nu}_\mu$ - e^- and $\bar{\nu}_\tau$ - e^- scattering at the one-loop level of accuracy is mandatory, in order to distinguish between the $\bar{\nu}_\mu$ and $\bar{\nu}_\tau$ events that originate from the reactor $\bar{\nu}_e \rightarrow \bar{\nu}_\mu$ and $\bar{\nu}_e \rightarrow \bar{\nu}_\tau$ oscillations.

In view of the fact that the behaviors of reactor antineutrino oscillations in a medium-baseline experiment are essentially insensitive to terrestrial matter effects¹⁾, we shall not take into account such insignificant corrections

in the following proof-of-concept analysis.

III. ELASTIC SCATTERING

The elastic scattering of $\bar{\nu}_\mu$ or $\bar{\nu}_\tau$ with an electron takes place via the standard weak neutral-current interactions as typically illustrated in Fig. 2, whereas that of $\bar{\nu}_e$ with an electron occurs through both neutral- and charged-current interactions. After all the one-loop radiative corrections have been taken into account [22–25], the differential cross sections of elastic $\bar{\nu}_e$ - e^- , $\bar{\nu}_\mu$ - e^- and $\bar{\nu}_\tau$ - e^- scattering reactions are found to be

$$\begin{aligned} \frac{d\sigma_e}{dT_e} &= \frac{2G_\mu^2 \rho^2 m_e}{\pi} \left[\kappa_e^2 s_W^4 + \left(1 - \frac{T_e}{E}\right)^2 \left(\frac{\rho-2}{2\rho} - \kappa_e s_W^2\right)^2 \right. \\ &\quad \left. + \frac{m_e T_e}{E^2} \kappa_e s_W^2 \left(\frac{\rho-2}{2\rho} - \kappa_e s_W^2\right) \right], \\ \frac{d\sigma_\mu}{dT_e} &= \frac{2G_\mu^2 \rho^2 m_e}{\pi} \left[\kappa_\mu^2 s_W^4 + \left(1 - \frac{T_e}{E}\right)^2 \left(\frac{1}{2} - \kappa_\mu s_W^2\right)^2 \right. \\ &\quad \left. + \frac{m_e T_e}{E^2} \kappa_\mu s_W^2 \left(\frac{1}{2} - \kappa_\mu s_W^2\right) \right], \\ \frac{d\sigma_\tau}{dT_e} &= \frac{2G_\mu^2 \rho^2 m_e}{\pi} \left[\kappa_\tau^2 s_W^4 + \left(1 - \frac{T_e}{E}\right)^2 \left(\frac{1}{2} - \kappa_\tau s_W^2\right)^2 \right. \\ &\quad \left. + \frac{m_e T_e}{E^2} \kappa_\tau s_W^2 \left(\frac{1}{2} - \kappa_\tau s_W^2\right) \right], \end{aligned} \quad (6)$$

where $T_e \equiv E_e - m_e$ stands for the recoil energy of the final-state electron, G_μ is the Fermi coupling constant determined from a precision measurement of the muon lifetime, m_e denotes the electron mass, E represents the initial neutrino energy, and $s_W \equiv \sin \theta_W$ with θ_W being the Weinberg angle. Moreover, the overall factor ρ in Eq. (6) is given by

$$\begin{aligned} \rho &= 1 + \frac{\alpha_{\text{em}}}{4\pi} \left\{ \frac{3}{4s_W^2} \ln c_W^2 - \frac{7}{4s_W^2} + \frac{2c_Z}{c_W^2 s_W^2} + G \left(c_W^2, \frac{m_h^2}{m_Z^2} \right) \right. \\ &\quad + \frac{1}{2m_W^2 s_W^2} \left[\sum_f m_f^2 \ln \left(\frac{m_f^2}{m_W^2} \right) \right. \\ &\quad - 2 \sum_{q,q'} |V_{qq'}|^2 \int_0^1 dx \left[m_q^2 x + m_{q'}^2 (1-x) \right] \\ &\quad \times \ln \left[\frac{m_q^2 x + m_{q'}^2 (1-x)}{m_W^2} \right] \\ &\quad \left. \left. - 2 \sum_\alpha \int_0^1 dx \left[m_\alpha^2 (1-x) \right] \ln \left[\frac{m_\alpha^2 (1-x)}{m_W^2} \right] \right] \right\}, \end{aligned} \quad (7)$$

where α_{em} denotes the electromagnetic fine-structure con-

¹⁾ In fact, only θ_{12} and F_{21} are slightly contaminated by terrestrial matter effects for a medium-baseline reactor antineutrino experiment like JUNO [18–20]. It is also known that the combination " $\sin 2\theta_{23} \sin \delta$ " is in particular insensitive to the matter-induced corrections [21].

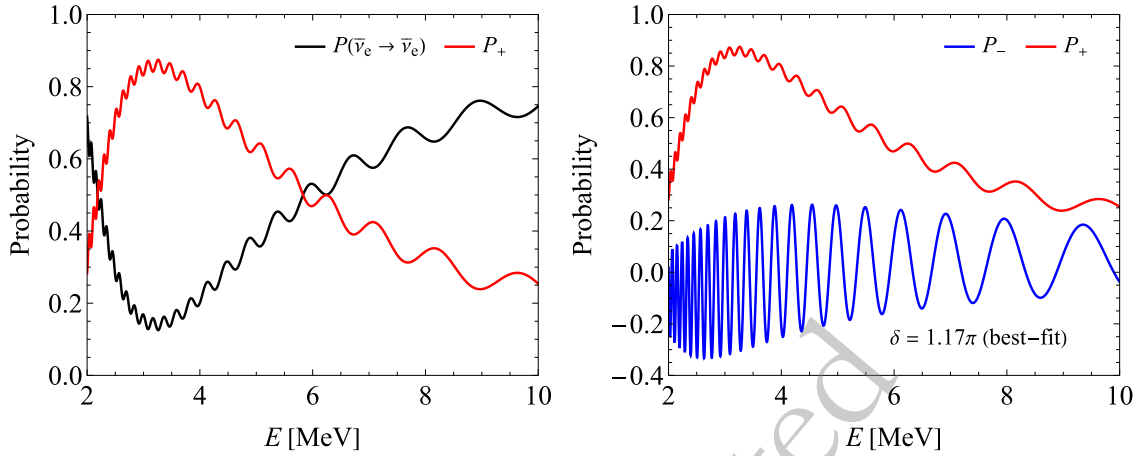


Fig. 1. (color online) The sum of the *appearance* oscillation probabilities $P_+ \equiv P(\bar{\nu}_e \rightarrow \bar{\nu}_\mu) + P(\bar{\nu}_e \rightarrow \bar{\nu}_\tau)$ versus the survival probability $P(\bar{\nu}_e \rightarrow \bar{\nu}_e)$ changing with the beam energy E is shown in the left panel, while P_+ and $P_- \equiv P(\bar{\nu}_e \rightarrow \bar{\nu}_\mu) - P(\bar{\nu}_e \rightarrow \bar{\nu}_\tau)$ in the right panel. The best-fit values of the relevant oscillation parameters $\sin^2 \theta_{12} = 0.308$, $\sin^2 \theta_{13} = 0.02215$, $\sin^2 \theta_{23} = 0.470$ and $\delta = 1.17\pi$, together with $m_2^2 - m_1^2 = 7.49 \times 10^{-5} \text{ eV}^2$ and $m_3^2 - m_1^2 = 2.513 \times 10^{-3} \text{ eV}^2$ (normal mass ordering) have been input [16, 17], and the baseline length is set to $L = 53 \text{ km}$.

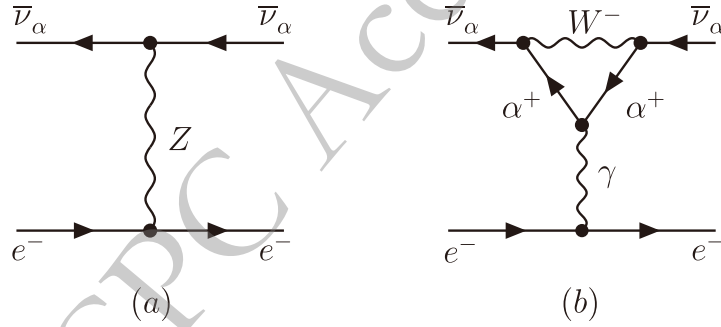


Fig. 2. The Feynman diagrams of elastic $\bar{\nu}_\alpha$ - e^- scattering (for $\alpha = \mu, \tau$) via weak neutral-current interactions: (a) the tree-level contribution; (b) the dominant one-loop contribution, where only one typical diagram is shown for illustration. It is the difference between the charged-lepton masses m_μ and m_τ that makes the $\bar{\nu}_\mu$ - e^- and $\bar{\nu}_\tau$ - e^- scattering cross sections distinguishable. Note that a full set of the one-loop Feynman diagrams will be taken into account in our analytical and numerical calculations of the $\bar{\nu}_\alpha$ - e^- scattering processes.

stant, m_h , m_W and m_Z stand respectively for the Higgs-, W - and Z -boson masses, m_f represents the charged-fermion mass, m_α refers to the charged-lepton mass, m_q and $m_{q'}$ are the respective up- and down-type quark masses, $c_W \equiv \cos \theta_W$, $V_{qq'}$ denote the elements of the Cabibbo-Kobayashi-Maskawa (CKM) quark flavor mixing matrix (for $q = u, c, t$ and $q' = d, s, b$), the coefficient c_Z and the function $G(c_W^2, x)$ are defined as

$$c_Z \equiv \frac{19}{8} - \frac{7}{2} s_W^2 + 3s_W^4, \\ G(c_W^2, x) \equiv \frac{3}{4} \cdot \frac{x}{s_W^2} \left[\frac{1}{c_W^2 - x} \ln \left(\frac{c_W^2}{x} \right) + \frac{1}{c_W^2(1-x)} \ln x \right], \quad (8)$$

and the summation over q and q' quarks in Eq. (7) should include their color factor "3". On the other hand, the flavor-dependent functions κ_α (for $\alpha = e, \mu, \tau$) are expressed as

$$\kappa_\alpha(q^2) = 1 - \left\{ \frac{c_W}{s_W} \cdot \frac{\Sigma_{AZ}(q^2)}{q^2} + \frac{c_W^2}{s_W^2} \text{Re} \left[\frac{\Sigma_Z(m_Z^2)}{m_Z^2} - \frac{\Sigma_W(m_W^2)}{m_W^2} \right] \right. \\ \left. - \frac{\alpha_{\text{em}}}{2\pi} \cdot \frac{c_W^2}{s_W^2} \left[\left(\frac{m_Z^2}{q^2} - 2 \right) \right. \right. \\ \left. \left. \times \left[\frac{1}{\epsilon} - \gamma_E + \ln 4\pi + \ln \left(\frac{\mu^2}{m_W^2} \right) \right] \right] \right. \\ \left. - \frac{1}{c_W^2} \left[\frac{c_A}{c_W^2} - R_\alpha(q^2) \right] \right\}, \quad (9)$$

where $q^2 = -2m_e T_e$ is the square of momentum transfer, and

$$c_A \equiv \frac{19}{8} - \frac{17}{4} s_W^2 + 3s_W^4, \\ R_\alpha(q^2) \equiv \frac{1}{3} + 2 \int_0^1 dx [x(1-x)] \ln \left[\frac{m_W^2}{m_\alpha^2 - q^2 x(1-x)} \right]. \quad (10)$$

In Eq. (9) the ultra-violet divergence term and the μ -dependence term stemming from dimensional regularization (with μ being the 't Hooft mass scale, $d \equiv 4 - 2\epsilon$ being the spacetime dimension and $\gamma_E \approx 0.577$ being the Euler-Mascheroni constant) will cancel the divergence terms associated with the one-loop self-energy functions of the gauge bosons $\Sigma_{AZ}(q^2)$, $\Sigma_W(m_W^2)$ and $\Sigma_Z(m_Z^2)$ [22].

It is obvious that switching off the one-loop radiative corrections is equivalent to taking $\rho = 1$ and $\kappa_e = \kappa_\mu = \kappa_\tau = 1$, from which the tree-level equality $\sigma_\mu = \sigma_\tau$ is simply obtained. Note that $R_\mu(q^2)$ and $R_\tau(q^2)$ arise respectively from the one-loop $\bar{\nu}_\mu - \bar{\nu}_\mu - \gamma$ and $\bar{\nu}_\tau - \bar{\nu}_\tau - \gamma$ vertices as typically illustrated by Fig. 2 (b), and their discrepancy is attributed to the difference between m_μ^2 and m_τ^2 as can be easily seen from Eq. (10). If the resulting discrepancy between elastic $\bar{\nu}_\mu - e^-$ and $\bar{\nu}_\tau - e^-$ scattering cross sections is observed from a reactor antineutrino oscillation experiment, it will allow us to probe or constrain the fine effects of leptonic CP violation and μ - τ interchange symmetry breaking as described by P_- in Eq. (4).

Let us proceed to calculate the rates of $\bar{\nu}_e$, $\bar{\nu}_\mu$ and $\bar{\nu}_\tau$ events at the far detector. The initial reactor electron antineutrinos are produced from the nuclear beta decays, and the fluxes of $\bar{\nu}_\alpha$ events originating from $\bar{\nu}_e \rightarrow \bar{\nu}_\alpha$ oscillations (for $\alpha = e, \mu, \tau$) with a baseline length L are given as

$$\phi_\alpha(E) = \frac{1}{4\pi L^2} \cdot P(\bar{\nu}_e \rightarrow \bar{\nu}_\alpha) \cdot \frac{dN'_e}{dE}, \quad (11)$$

where dN'_e/dE is the rate for the initial $\bar{\nu}_e$ events. In the far detector, the event rates of elastic $\bar{\nu}_\alpha + e^- \rightarrow \bar{\nu}_\alpha + e^-$ scattering turn out to be

$$\begin{aligned} \frac{dN_\alpha}{dT'_e} &= N_T T \int_0^\infty dT_e \frac{1}{\sqrt{2\pi} \delta T_e} \\ &\times \exp \left[-\frac{(T_e - T'_e)^2}{2(\delta T_e)^2} \right] \int_{E_{\min}}^\infty dE \frac{d\sigma_\alpha}{dT_e} \phi_\alpha, \quad (12) \end{aligned}$$

where N_T is the total number of the target electrons in the far detector, T denotes the operation duration, T'_e represents the observed energy in the detector corresponding to the electron recoil energy T_e and the energy resolution δT_e with a Gaussian distribution, the differential cross sections $d\sigma_\alpha/dT_e$ and the fluxes ϕ_α have been given in Eqs. (6) and (11) respectively.

To see the flavor effects in a clear way, we rewrite the integrand of the second integral in Eq. (12) and sum over the flavor index α . Then we are left with

$$\begin{aligned} \sum_\alpha \frac{d\sigma_\alpha}{dT_e} \phi_\alpha &= \frac{1}{4\pi L^2} \cdot \frac{dN'_e}{dE} \left[P(\bar{\nu}_e \rightarrow \bar{\nu}_e) \frac{d\sigma_e}{dT_e} \right. \\ &\quad \left. + \frac{P_+}{2} \left(\frac{d\sigma_\mu}{dT_e} + \frac{d\sigma_\tau}{dT_e} \right) + \frac{P_-}{2} \left(\frac{d\sigma_\mu}{dT_e} - \frac{d\sigma_\tau}{dT_e} \right) \right], \quad (13) \end{aligned}$$

where the expressions of P_\pm have been given in Eq. (4). Since the $\bar{\nu}_e$ contribution can be subtracted from the total elastic scattering events by accurately measuring the $\bar{\nu}_e$ flux via the inverse beta decay $\bar{\nu}_e + p \rightarrow e^+ + n$, we are therefore able to observe the appearance of $\bar{\nu}_\mu$ and $\bar{\nu}_\tau$ events as a whole. In other words, it is relatively easy to extract P_+ from such a precision measurement, and extracting the information on P_- will be very challenging. But the latter is highly nontrivial and deserves to be carefully studied, simply because it may open a new window to probe or constrain leptonic CP violation in the reactor-based experiments.

To illustrate, let us specify the nominal setup for a reactor antineutrino experiment by taking the JUNO detector for example, and calculate the elastic $\bar{\nu}_\alpha - e^-$ scattering event rates (for $\alpha = e, \mu, \tau$). Given the total thermal power P_{th} of the chosen nuclear reactors, the production rate of the reactor electron antineutrinos can be calculated by use of

$$\frac{dN'_e}{dE} = \frac{P_{\text{th}}}{\sum_i f_i \epsilon_i} \sum_i f_i S_i(E), \quad (14)$$

where the subscript "i" refers to the radioactive isotopes ^{235}U , ^{238}U , ^{239}Pu and ^{241}Pu , f_i stands for the average fraction of each isotope, and ϵ_i denotes the thermal energy released per fission. The energy spectrum $S_i(E)$ of $\bar{\nu}_e$ from the beta decays of fission products is obtained with the help of a fifth-power fitting formula [26]. We assume $P_{\text{th}} = 26.6$ GW, $f_i = \{0.561, 0.076, 0.307, 0.056\}$ and $\epsilon_i = \{202.36, 205.99, 211.12, 214.26\}$ MeV as the typical inputs in our numerical calculation¹⁾, and use the values of α_{ij} from Ref. [26]. Then the elastic scattering event rates at the far detector can be calculated by convolving the antineutrino fluxes and the differential cross sections, given the total number of target electrons $N_T \approx 6.72 \times 10^{33}$ corresponding to the 12% mass fraction of hydrogen and 88% of carbon in the 20 kiloton liquid scintillator. We show the final numerical results in Fig. 3. Some comments are in order.

• In the left panel, the contribution to the event rate in Eq. (12) from the last term on the right-hand side of Eq. (13) has been illustrated, where the dependence on the

1) Note that $1 \text{ GW} = 6.2415 \times 10^{21} \text{ MeV} \cdot \text{s}^{-1}$ holds.

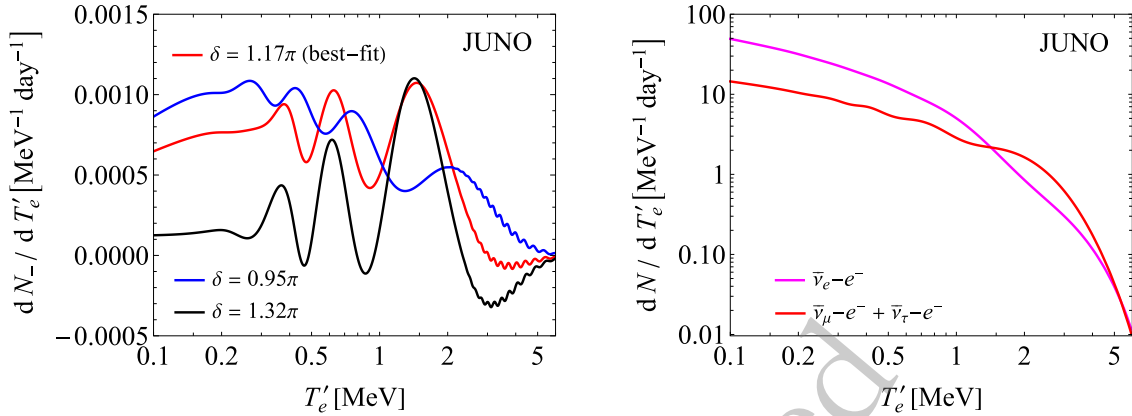


Fig. 3. (color online) In the left panel, the δ -dependent contribution $P_- (\mathrm{d}\sigma_\mu/\mathrm{d}T'_e - \mathrm{d}\sigma_\tau/\mathrm{d}T'_e)/2$ to the event rate is denoted as $\mathrm{d}N_-/\mathrm{d}T'_e$, and its numerical result is illustrated by inputting the best-fit value $\delta = 1.17\pi$ and its 1σ lower (upper) bound $\delta = 0.95\pi$ (1.32π). In the right panel, the event rate $\mathrm{d}N_e/\mathrm{d}T'_e$ for $\bar{\nu}_e-e^-$ scattering and the sum $\mathrm{d}N_\mu/\mathrm{d}T'_e + \mathrm{d}N_\tau/\mathrm{d}T'_e$ of the event rates for $\bar{\nu}_\mu-e^-$ and $\bar{\nu}_\tau-e^-$ scattering are presented. Here the JUNO detector with 20 kiloton liquid scintillator and an effective energy resolution $\delta T_e/T_e = 3\%/\sqrt{T_e/\text{MeV}}$ have been taken into consideration.

CP-violating phase δ is evident. For simplicity, we take the best-fit value $\delta = 1.17\pi$ and its 1σ lower (upper) bound $\delta = 0.95\pi$ (1.32π) from Ref. [16]. Note that this best-fit result agrees perfectly with $\delta = 1.20\pi$ obtained from Ref. [17] in the case of normal neutrino mass ordering. Although $\mathrm{d}N_-/\mathrm{d}T'_e$ is very sensitive to the values of δ , the variation of the event rates at the JUNO turns out to be $0.001 \text{ MeV}^{-1}\text{day}^{-1}$ at most. As indicated in Eq. (13), the suppression arises mainly from the difference between the one-loop cross sections for $\bar{\nu}_\mu-e^-$ and $\bar{\nu}_\tau-e^-$ scattering. The ratio of such a difference to the tree-level cross section is about 1%, while the oscillation probability difference P_- contributes some extra suppression. An experimental determination of the event rate at the level of $0.001 \text{ MeV}^{-1}\text{day}^{-1}$ is no doubt a big challenge.

- In the right panel, the sum $\mathrm{d}N_\mu/\mathrm{d}T'_e + \mathrm{d}N_\tau/\mathrm{d}T'_e$ over the event rates for $\bar{\nu}_\mu-e^-$ and $\bar{\nu}_\tau-e^-$ scattering is presented together with $\mathrm{d}N_e/\mathrm{d}T'_e$ for $\bar{\nu}_e-e^-$ scattering. Below $T'_e \approx 1.5 \text{ MeV}$, the $\bar{\nu}_e$ event rate is always dominant. However, for $T'_e > 1.5 \text{ MeV}$, we have more $\bar{\nu}_\mu$ and $\bar{\nu}_\tau$ events. This observation can be easily understood as follows. The oscillation probability P_+ is larger than $P(\bar{\nu}_e \rightarrow \bar{\nu}_e)$ for the antineutrino beam energy $E \in [2, 6] \text{ MeV}$, indicating that more $\bar{\nu}_\mu$ and $\bar{\nu}_\tau$ events than $\bar{\nu}_e$ arrive in the far detector. As mentioned before, the $\bar{\nu}_e$ flux will be precisely measured through the inverse beta decay such that its contribution to the elastic scattering events can be reliably subtracted. For the visible energy $T'_e \in [0.1, 4] \text{ MeV}$, the appearance of $\bar{\nu}_\mu$ and $\bar{\nu}_\tau$ at the JUNO could be optimistically demonstrated by observing the elastic scattering events at the rate of $(1 \cdots 10) \text{ MeV}^{-1}\text{day}^{-1}$.

Within the energy region $T'_e \in [0.1, 4] \text{ MeV}$, a number

of backgrounds for observing the recoiled electrons should be taken into account, including the internal background due to the radioactivity of contaminants in the scintillator, the external backgrounds from the γ radioactivity of surrounding materials and beta decays of cosmogenic isotopes from the spallation of cosmic muons. According to the background analysis for the detection of solar neutrinos at the JUNO [27], in an ideal radiopurity scenario, the largest internal background comes from the ^{210}Pb chain and the ^{238}U chain with a total rate about 419 counts per kiloton per day in the range $T'_e \in [0.45, 1.6] \text{ MeV}$. The external γ background can be eliminated by only retaining the events within the spherical fiducial volume of a radius about 15 meters. The cosmogenic background is dominated by the beta decays of ^{11}C at a rate of about 1761 counts per kiloton per day. In addition, the solar neutrinos themselves serve as an irreducible background, where the dominant contribution of 500 counts per kiloton per day is made by ^7Be neutrinos. Obviously, the background rate is much larger than the signal rate associated with the flavor oscillations of reactor antineutrinos. One possible way out is to implement the directional information on the recoiled electrons such that the antineutrinos coming from the direction opposite to the nuclear reactors can be distinguished from the others.

Furthermore, the dependence on the leptonic CP-violating phase δ at the per-mille level will be relevant if the statistical uncertainty in the total number of $\bar{\nu}_\mu-e^-$ and $\bar{\nu}_\tau-e^-$ scattering events reaches the same level, i.e., with 10^6 events. This can be realized by increasing the thermal power of reactors, optimizing the baseline in order to enhance the CP-violating effect and the antineutrino fluxes, and even constructing a much larger far detector.

IV. SUMMARY

We have carried out a *proof-of-concept* study of the possibility to observe the appearance of $\bar{\nu}_\mu$ and $\bar{\nu}_\tau$ events in the far detector of a reactor antineutrino oscillation experiment. Taking the JUNO experiment for example, we have calculated the differential event rate for $\bar{\nu}_\mu$ - e^- and $\bar{\nu}_\tau$ - e^- scattering and find that the total rate is about 9 counts per day for a 20 kiloton liquid-scintillator detector, while that for $\bar{\nu}_e$ - e^- scattering is about 17 counts per day. However, the $\bar{\nu}_e$ events can be eliminated by precisely measuring the $\bar{\nu}_e$ flux through the inverse beta decay $\bar{\nu}_e + p \rightarrow e^+ + n$. We stress that it is important to experimentally verify the appearance of $\bar{\nu}_\mu$ and $\bar{\nu}_\tau$ events, so as to test the conservation of probability for reactor antineutrino oscillations.

When the one-loop correction to the cross sections for

antineutrino-electron scattering is taken into account, the event rate becomes dependent on the leptonic CP-violating phase δ through the oscillation probability difference $P_- \equiv P(\bar{\nu}_e \rightarrow \bar{\nu}_\mu) - P(\bar{\nu}_e \rightarrow \bar{\nu}_\tau)$. Such dependence relies on both a nonzero P_- and the difference in the cross sections of elastic $\bar{\nu}_\mu$ - e^- and $\bar{\nu}_\tau$ - e^- scattering, and hence it is highly suppressed. That is why we expect that an unprecedented precision measurement of elastic antineutrino-electron scattering events at the per-mille level is required to probe or constrain leptonic CP violation in the foreseeable future.

ACKNOWLEDGMENTS

The authors are indebted to Jihong Huang for his kind technical helps and valuable discussions.

References

- [1] Y. F. Wang, *Nuovo Cim. C* **037**(03), 65 (2014)
- [2] L. J. Wen, J. Cao and Y. F. Wang, *Ann. Rev. Nucl. Part. Sci.* **67**, 183 (2017), arXiv: 1803.10162 [hep-ex]
- [3] C. L. Cowan, F. Reines, F. B. Harrison, H. W. Kruse and A. D. McGuire, *Science* **124**, 103 (1956)
- [4] K. Eguchi *et al.* [KamLAND], *Phys. Rev. Lett.* **90**, 021802 (2003), arXiv: hep-ex/0212021 [hep-ex]
- [5] F. P. An *et al.* [Daya Bay], *Phys. Rev. Lett.* **108**, 171803 (2012), arXiv: 1203.1669 [hep-ex]
- [6] J. K. Ahn *et al.* [RENO], *Phys. Rev. Lett.* **108**, 191802 (2012), arXiv: 1204.0626 [hep-ex]
- [7] F. An *et al.* [JUNO], *J. Phys. G* **43**(3), 030401 (2016), arXiv: 1507.05613 [physics.ins-det]
- [8] A. Abusleme *et al.* [JUNO], *Prog. Part. Nucl. Phys.* **123**, 103927 (2022), arXiv: 2104.02565 [hep-ex]
- [9] Z. z. Xing and S. Zhou, Zhejiang University Press and Springer-Verlag, 2011.
- [10] B. Pontecorvo, *Sov. Phys. JETP* **6** (1957) 429 [*Zh. Eksp. Teor. Fiz.* **33** (1957) 549].
- [11] Z. Maki, M. Nakagawa and S. Sakata, *Prog. Theor. Phys.* **28**, 870 (1962)
- [12] M. Blennow, E. Fernández-Martínez, J. Hernández-García, J. López-Pavón, X. Marciano and D. Naredo-Tuero, *JHEP* **08**, 030 (2023), arXiv: 2306.01040 [hep-ph]
- [13] C. Jarlskog, *Phys. Rev. Lett.* **55**, 1039 (1985)
- [14] D. d. Wu, *Phys. Rev. D* **33**, 860 (1986)
- [15] Z. z. Xing and Z. h. Zhao, *Rept. Prog. Phys.* **79**(7), 076201 (2016), arXiv: 1512.04207 [hep-ph]
- [16] I. Esteban, M. C. Gonzalez-Garcia, M. Maltoni, I. Martinez-Soler, J. P. Pinheiro and T. Schwetz, *JHEP* **12**, 216 (2024), arXiv: 2410.05380 [hep-ph]
- [17] F. Capozzi, W. Giarè, E. Lisi, A. Marrone, A. Melchiorri and A. Palazzo, *Phys. Rev. D* **111**(9), 093006 (2025), arXiv: 2503.07752 [hep-ph]
- [18] Y. F. Li, Y. Wang and Z. z. Xing, *Chin. Phys. C* **40**(9), 091001 (2016), arXiv: 1605.00900 [hep-ph]
- [19] Y. F. Li, Z. z. Xing and J. y. Zhu, *Phys. Lett. B* **782**, 578 (2018), arXiv: 1802.04964 [hep-ph]
- [20] F. Capozzi, E. Lisi and A. Marrone, *Phys. Rev. D* **102**(5), 056001 (2020), arXiv: 2006.01648 [hep-ph]
- [21] S. Toshev, *Mod. Phys. Lett. A* **6**, 455 (1991)
- [22] W. J. Marciano and A. Sirlin, *Phys. Rev. D* **22**, 2695 (1980) [erratum: *Phys. Rev. D* **31**, 213 (1985)]
- [23] S. Sarantakos, A. Sirlin and W. J. Marciano, *Nucl. Phys. B* **217**, 84 (1983)
- [24] J. Huang and S. Zhou, *Phys. Rev. D* **108**(9), 093010 (2023), arXiv: 2307.04685 [hep-ph]
- [25] J. Huang and S. Zhou, *Phys. Rev. D* **111**(3), 033005 (2025), arXiv: 2412.17047 [hep-ph]
- [26] T. A. Mueller, *et al.*, *Phys. Rev. C* **83**, 054615 (2011), arXiv: 1101.2663 [hep-ex]
- [27] A. Abusleme *et al.* [JUNO], *JCAP* **10**, 022 (2023), arXiv: 2303.03910 [hep-ex]